



**The Abdus Salam  
International Centre for Theoretical Physics**



**1953-21**

**International Workshop on the Frontiers of Modern Plasma Physics**

*14 - 25 July 2008*

**Magnetic Reconnection in Collisionless Regimes.**

D. Grasso  
*Politecnico di Torino  
Dip. di Energetica  
Italy*

# Magnetic Reconnection in Collisionless Regimes



Daniela Grasso

Politecnico di Torino, Italy

*International Workshop on the Frontiers of Modern Plasma Physics*

*ICTP, Trieste, July 14-25, 2008*

# Outline

---

## CONCEPTS:

- Magnetic reconnection:
  - Phenomenology
  - Theory: the MagnetoHydroDynamic model
  - Ideal and nonideal Ohm's law
  - The resistive paradigm
- The problem of fast reconnection: the collisionless regime

## RESULTS:

- The two-field model:
  - 2D limit: the cold and hot electron regimes at low  $\beta$
  - 3D effects
- The 2D four-field model:
  - The finite  $\beta$  regime
- Conclusions & open problems

# Phenomenology

---

- Magnetic reconnection is a process which takes place in conducting fluids and plasmas.
- It's a topological variation of the magnetic field, accompanied by a fast release of magnetic energy into heat and ordered kinetic energy.
- It's a local process which causes global changes.
- It's typically accompanied by the formation of intense current density layers.

# Phenomenology

- Sawtooth oscillations in laboratory plasmas: relaxation oscillations of density and temperature, in the center of the plasma:

1. abrupt loss of energy confinement
2. quenching of the plasma heating

- Typical time scale of order of 100 microseconds.

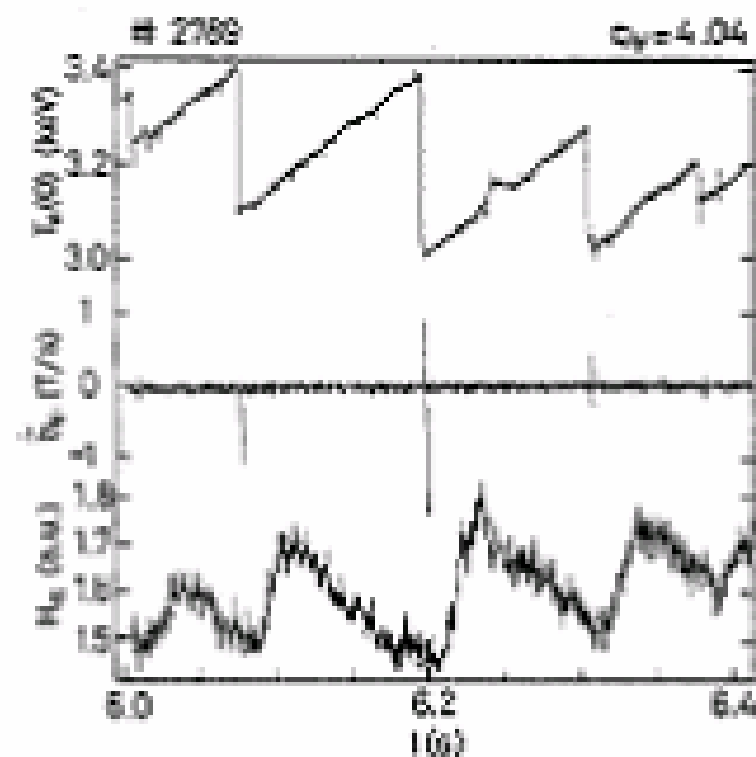
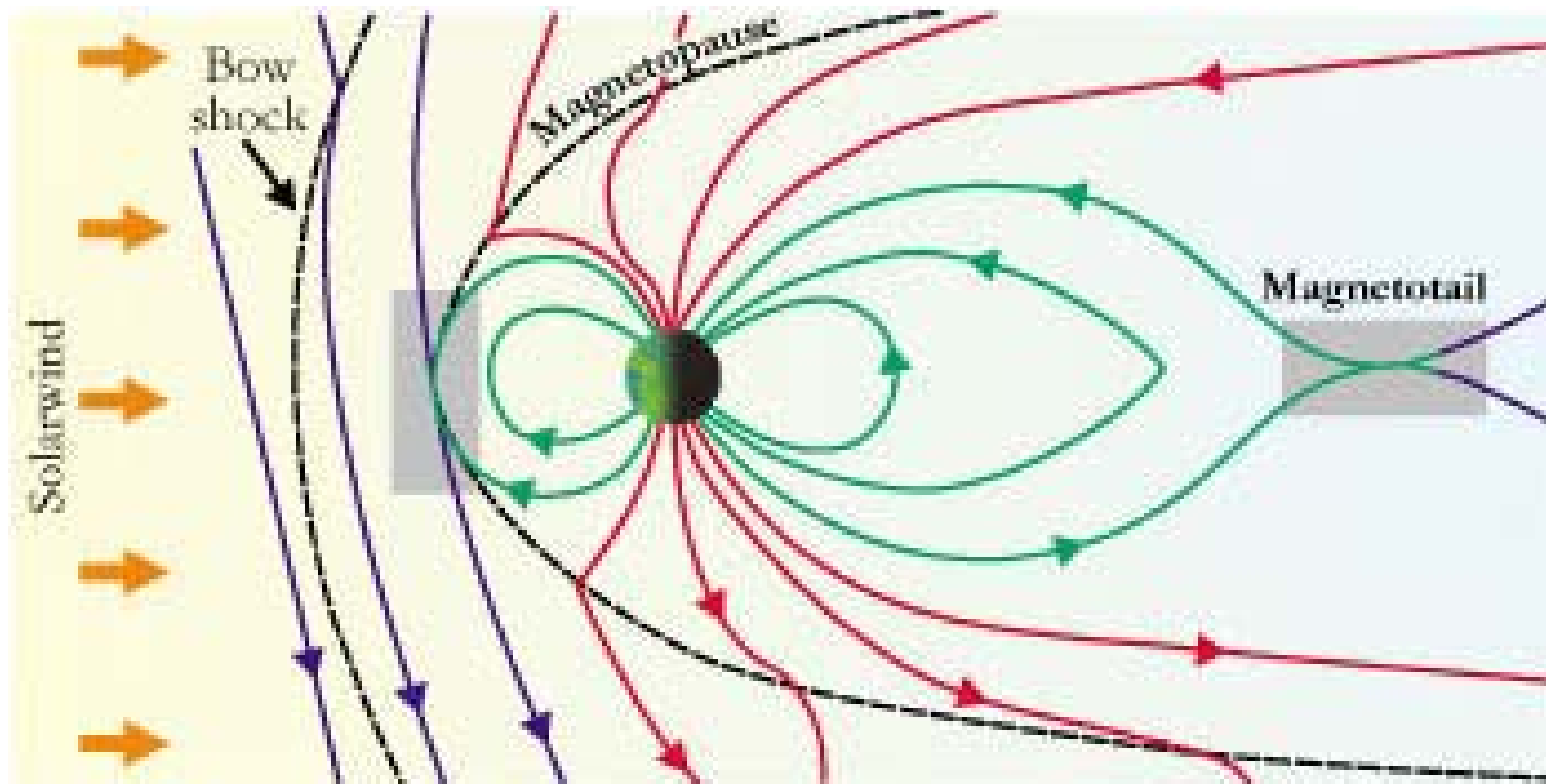


FIG. 2. Evidence of 'spikes' on the magnetic signal correlated with the central temperature collapse of the sawtooth. The maximum of the  $B_z$  signal (indicative of the heat pulse reaching the edge) occurs much later.

# Phenomenology

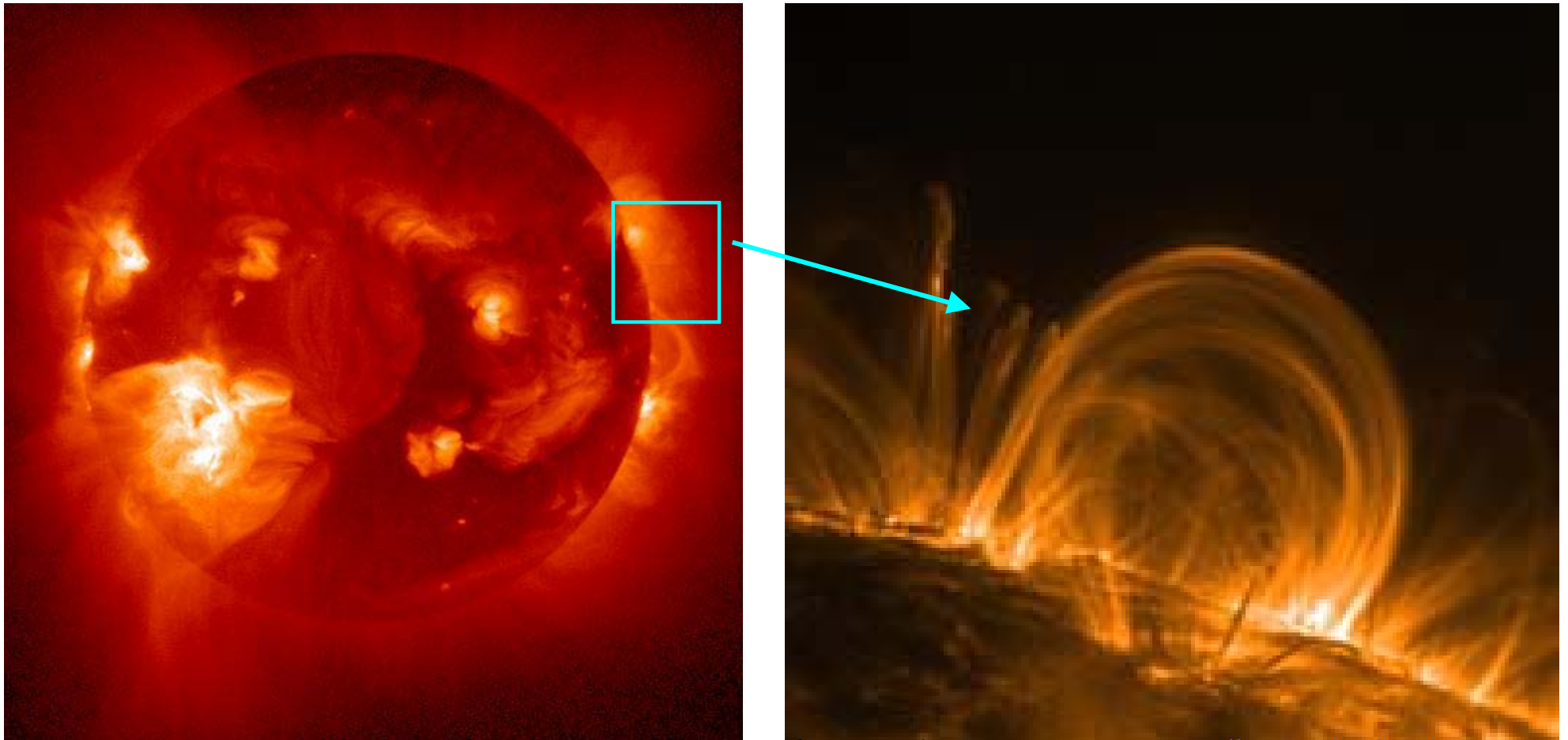
- **Earth's Magnetosphere:** the region of space to which the Earth's magnetic field is confined by the solar wind plasma blowing outward from the Sun.



The ESA mission  
"Cluster"  
observed  
reconnection in  
the earth  
magnetotail  
(C.J. Xiao *et al.*,  
Nature Physics,  
July 2006).

# Phenomenology

- Solar flares: tremendous explosions on the surface of the Sun. In a few minutes (100 to 1000 secs) as much energy as  $10^{32}$  ergs is released. They occur near sunspots, usually along a neutral line.



Source: Yohkoh and Trace missions web sites ([www.isas.jaxa.jp/home/solar/](http://www.isas.jaxa.jp/home/solar/) and [www.nasa.gov/missions](http://www.nasa.gov/missions))

# Theory: the MHD model

- The MagnetoHydroDynamic model treats the plasma as a single fluid.

$$\rho = \sum_{\alpha} n_{\alpha} m_{\alpha}$$

$$\vec{v} = \frac{\sum_{\alpha} n_{\alpha} m_{\alpha} \vec{v}_{\alpha}}{\sum_{\alpha} n_{\alpha} m_{\alpha}}$$

$$\alpha = i, e$$

$$p = \sum_{\alpha} p_{\alpha}$$

$$\vec{J} = \sum_{\alpha} n_{\alpha} \mathbf{q}_{\alpha} \vec{v}_{\alpha}$$

- MHD description is a rough approximation to describe large scale and low frequency phenomena.

# The MHD model

$$\frac{\partial \rho}{\partial t} + \nabla \cdot \rho \vec{v} = 0$$

$$\rho \left( \frac{\partial \vec{v}}{\partial t} + \vec{v} \cdot \nabla \vec{v} \right) = \frac{\vec{J} \times \vec{B}}{c} - \nabla p$$

$$\frac{d}{dt} \left( \frac{p}{\rho^\gamma} \right) = 0, \quad \nabla \cdot \vec{v} = 0$$

Continuity equation

Motion Equation

Closure

$$\nabla \times \vec{E} = -\frac{1}{c} \frac{\partial \vec{B}}{\partial t}$$

$$\nabla \times \vec{B} = \frac{4\pi}{c} \vec{J}$$

$$\nabla \cdot \vec{B} = 0$$

$$\nabla \cdot \vec{E} = 0$$

Maxwell equation  
+  
Quasineutrality

Resistive MHD

$$\vec{E} + \frac{\vec{v} \times \vec{B}}{c} = \eta \vec{J}$$

Ohm's law

# Ideal Ohm's law

$$\vec{E} + \frac{\vec{v} \times \vec{B}}{c} = 0$$

$$\frac{\partial \vec{B}}{\partial t} + \nabla \times (\vec{B} \times \vec{v}) = 0 \quad \rightarrow \quad \frac{\partial}{\partial t} \int_S \vec{B} \cdot d\vec{S} + \oint_C \vec{B} \cdot (\vec{v} \times d\vec{l}) = 0$$

The total variation of the magnetic flux  $\Phi = \int_S \vec{B} \cdot d\vec{S}$  through a surface in motion with the fluid is conserved.

**Frozen-in condition:** two fluid elements connected by a field line at a given time stay connected at later times.

# Ideal Ohm's law

- A 2D example

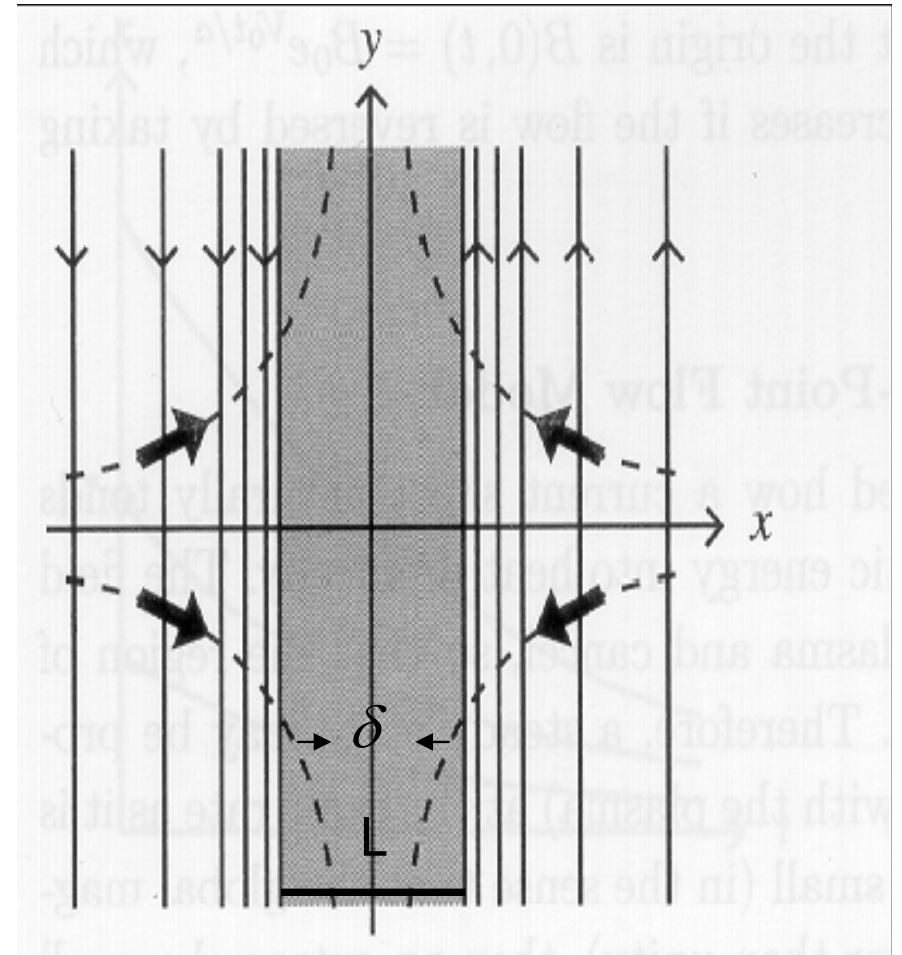
$$\vec{B} = B(x)\vec{e}_y \approx \frac{B_0 x}{L}$$

$$\nabla \times \vec{B} = \frac{4\pi}{c} \vec{J} \Rightarrow J_z \approx \frac{B_0}{L}$$

$$\vec{J} \times \vec{B} \approx \frac{B_0 x}{L^2}$$

$$L \rightarrow \delta \Rightarrow J_z \rightarrow B_0 / \delta$$

$$\delta \rightarrow 0 \Rightarrow \vec{J} \times \vec{B} \rightarrow \infty$$



# Non ideal Ohm's law

$$\vec{E} + \frac{\vec{v} \times \vec{B}}{c} \neq 0$$

In a non ideal plasma the frozen-in condition can be broken on a local scale, allowing motions otherwise forbidden. Magnetic field lines diffuse across the plasma and change their topology.

$$\frac{\partial \vec{B}}{\partial t} + \nabla \times (\vec{B} \times \vec{v}) \neq 0$$

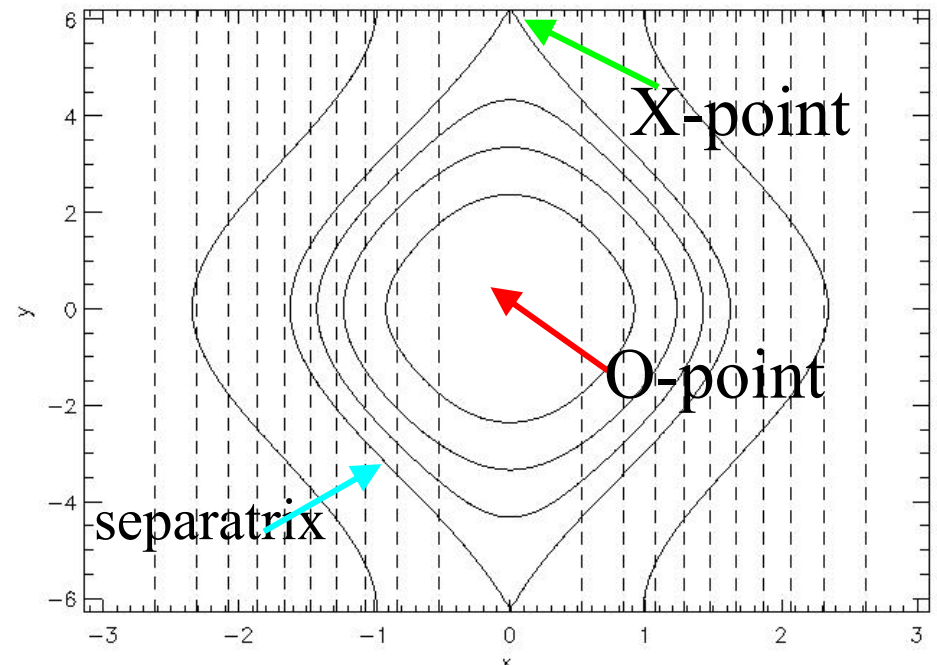
$$\vec{B} = \nabla \psi(x, y) \times \vec{e}_z$$

$$\vec{B} \cdot \nabla \psi = 0$$

Magnetic field lines are tangent to surfaces where  $\psi$  is constant

The magnetic flux function is the Hamiltonian for magnetic field lines

$$\dot{x} = \frac{\partial \psi}{\partial y} = B_x; \quad \dot{y} = -\frac{\partial \psi}{\partial x} = B_y$$



Magnetic island<sub>11</sub>

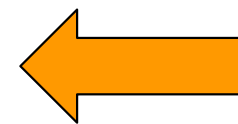
# The resistive MHD

- The characteristic time for propagation of phenomena in the MHD model is the Alfvén time  $\tau_A = L / V_A$  where

$V_A = B / \sqrt{4\pi m_i n_i}$  is the Alfvén velocity.

- Normalizing the equation of evolution of the magnetic field

$$\frac{\partial \vec{B}}{\partial t} + \nabla \times (\vec{B} \times \vec{v}) = \frac{1}{S} \nabla^2 \vec{B}$$



Singular  
perturbation

$$S = \frac{\tau_\eta}{\tau_A} \quad (10^7 \text{ Tokamak; } 10^{12} \text{ Solar corona})$$

$$\tau_\eta = L / D_m$$

$$D_m = \frac{\eta c^2}{4\pi} \quad 12$$

# The reduced RMHD

- 2D slab model with strong guide field along the ignorable direction

$$\vec{B} = B_0 \vec{e}_z + \nabla \psi_{eq}(x) \times \vec{e}_z$$

- MHD equations can be reduced to:

$$\frac{\partial \psi}{\partial t} + [\varphi, \psi] = -\varepsilon_\eta J$$

$$\frac{\partial U}{\partial t} + [\varphi, U] = [J, \psi]$$

$$U = \nabla^2 \varphi \quad J = -\nabla^2 \psi$$

$$\vec{V} = \vec{e}_z \times \nabla \varphi$$

$$[f, g] = \vec{e}_z \cdot \nabla f \times \nabla g$$

# The reduced RMHD

---

- Linear theory: the problem can be solved by standard asymptotic matching techniques, identifying an inner and an outer region.  
FKR, Phys. Fluids 1963
- The most important linear result is the determination of a threshold for the instability to occur

$$\Delta' = [\psi'_{out}(0^+) - \psi'_{out}(0^-)] / \psi_{out}(0) > 0$$

- It turns out that the low mode numbers are the most unstable.

# The problem of fast reconnection

The main problem in magnetic reconnection is the rate at which magnetic energy in a plasma can be converted into heat and ordered kinetic energy in a relatively short time.

$$\vec{E} + \frac{\vec{v} \times \vec{B}}{c} = \eta \vec{J} + \frac{m_e}{ne^2} \left( \frac{\partial \vec{J}}{\partial t} + \vec{v} \cdot \nabla \vec{J} \right) - \frac{1}{ne} \nabla p_e + \dots$$

$$\eta = m_e \nu_{ei} / ne^2 \propto T^{-3/2} \quad d_e = \frac{c}{\omega_{pe}} \approx m_e^{1/2} \quad \rho_s = \left( \frac{T_e}{T_i} \right)^{1/2} \rho_i$$

Resistivity

Electron

Ion sound

skin depth

Larmor radius

# The problem of fast reconnection

---

- At high temperature, such as in a fusion experiment, resistivity is very low.
- Discrepancies between theoretical predictions based on the resistive MHD and typical today's large experiments values brought the attention to electron inertia.
- From Sweet-Parker model (**Wesson 1990**) for the Jet parameters:

$$\tau_{res} \approx 3ms ; \quad \tau_{de} \approx 300\mu s$$

- Electron inertia drives the reconnection process providing the effective impedance to the parallel electric field, relaxing the frozen-in condition. The plasma flows through the reconnection region where the parallel electric field is non zero. So electrons are accelerated. The combined effects of the finite electron mass with the finite time in which the region is crossed, limits the current and allow for decoupling of the plasma motion from the magnetic field line motion. The role of the electron-ion collision frequency is played now by the inverse of the time in which the reconnection region is crossed.

# The two-field model

- The model by **Schep & Pegoraro (PoP 1994)** valid in slab geometry and low  $\beta$  plasma has been extensively investigated in the last decade.

- The magnetic field is assumed with a strong uniform component along the z-direction:

$$B = B_0 \vec{e}_z + \nabla \psi_{eq}(x) \times \vec{e}_z$$

- Equations normalized to a macroscopic scale length,  $L$ , and to  $\tau_A$  are:

$$\frac{\partial(\psi + d_e^2 J)}{\partial t} + [\varphi, \psi + d_e^2 J] - \rho_s^2 [U, \psi] = \frac{\partial(\varphi - \rho_s^2 U)}{\partial z}$$

Ohm's law

$$\frac{\partial U}{\partial t} + [\varphi, U] - [J, \psi] = -\frac{\partial J}{\partial z}$$

Momentum equation

$$U = \nabla \times \vec{v} = \nabla_{\perp}^2 \varphi; \quad \vec{v} = \vec{e}_z \times \nabla \varphi$$

$$J = -\nabla_{\perp}^2 \psi \quad [f, g] = \vec{e}_z \cdot \nabla f \times \nabla g$$

# The two-field model

- The above equations can be combined in terms of generalized flux and stream functions:

$$G_{\pm} = \psi + d_e^2 J \pm \rho_s^2 U, \quad \varphi_{\pm} = \varphi \pm \frac{\rho_s}{d_e} \psi$$

$$\frac{\partial G_{\pm}}{\partial t} + [\varphi_{\pm}, G_{\pm}] = \frac{\partial [\varphi_{\pm} \mp (\rho_s / d_e) G_{\pm}]}{\partial z}$$

$$\psi + d_e^2 J = (G_+ + G_-) / 2$$

$$d_e \rho_s U = (G_+ - G_-) / 2$$

**Energy**  
**is**  
**conserved!**

$$E = \int \left( |\nabla \psi|^2 + |\nabla \varphi|^2 + d_e^2 J^2 + \rho_s^2 U^2 \right) dV$$

↑	↑	↑	↑
$E_{\text{mag}}$	$E_{\text{Ki}}$	$E_{\text{Ke}}$	$E_{\text{Pe}}$

# Numerical results

Collaborators: D. Borgogno,  
F. Califano, D. Farina, F. Pegoraro,  
F. Porcelli, E. Tassi

- The above system has been investigated in the large  $\Delta'$  regime.
- Symmetric and asymmetric equilibria for the magnetic flux function have been chosen. Typically:

$$\psi_{eq} = \log(\cosh(x)); \quad \psi_{eq} = \frac{1}{\cosh^2(x)}; \quad \psi_{eq} = \log(\cosh(x)) + \alpha x; \quad \varphi_{eq} = 0$$

- Perturbations have been chosen in the following way:

$$\delta J(x, y, z; t)_{t=0} = \delta \hat{J}_1(x) \exp(ik_y y + ik_{z1} z) + \delta \hat{J}_2(x) \exp(ik_y y + ik_{z2} z)$$

where  $k_y = 2\pi m / L_y$ ,  $k_z = 2\pi n / L_z$  and  $(m, n)$  are the wave numbers

and  $\delta \hat{J}_{1,2}$  are localized within a width of order  $d_e$  around  $x_{s1, s2}$

- A 2D mode has  $K_z=0$ . Single helicity (SH) modes have  $K_{z1}=K_{z2}=K_z$  and evolve conserving the initial helicity  $K_z/K_y$  and are, thereof, equivalent to 2D modes.
- Multiple helicity modes (MH) correspond to a 3D setting.

# 2D limit

Reconnection time is of order of the inverse linear growth time.

Some numbers: for typical parameters of present day fusion experiments close to thermonuclear breakeven conditions, such as JET

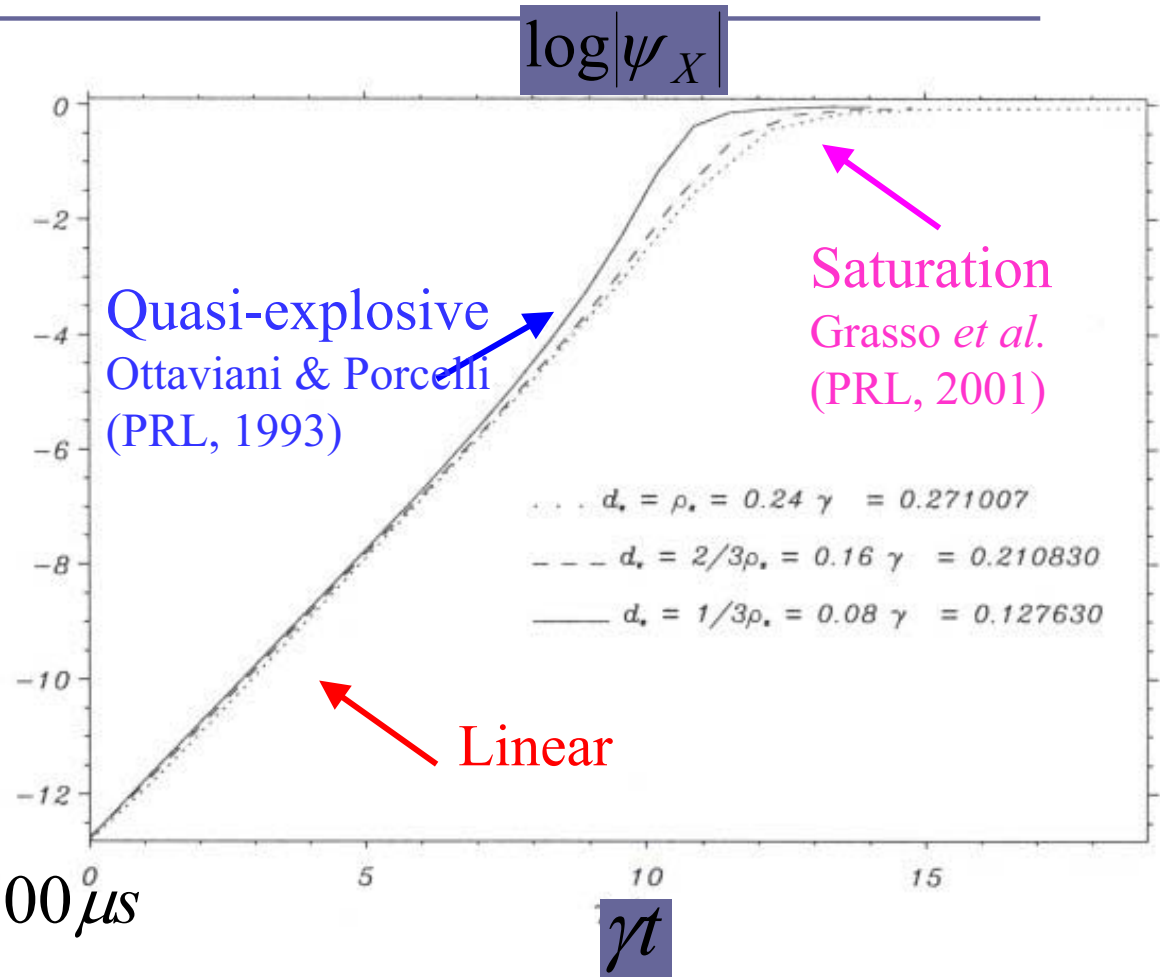
$$L_x \approx 0.5m; \quad \rho_s \approx 0.5cm;$$

$$d_e \approx 0.1cm; \quad \tau_A \approx 1\mu s$$

$$\tau_{growth} \approx \gamma_L^{-1} \tau_A$$

$$\tau_{growth} \approx \left(\frac{L_x}{\rho_s}\right)^{2/3} \left(\frac{L_x}{d_e}\right)^{1/3} \tau_A \leq 100 \mu s$$

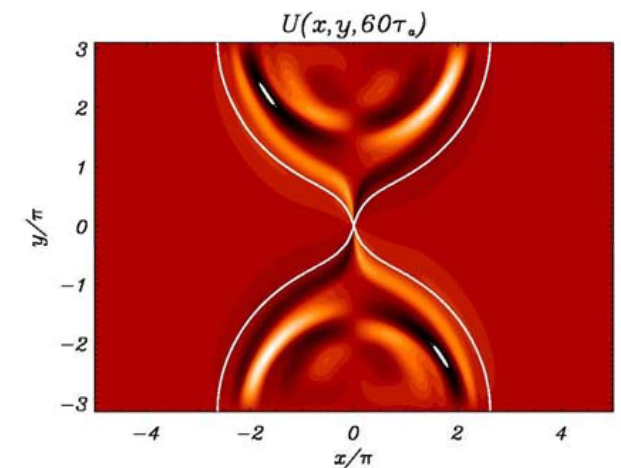
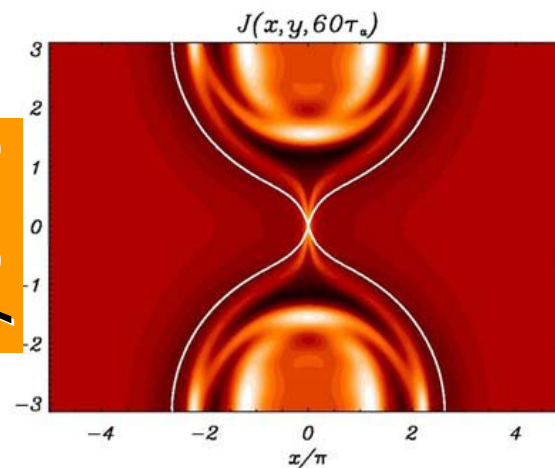
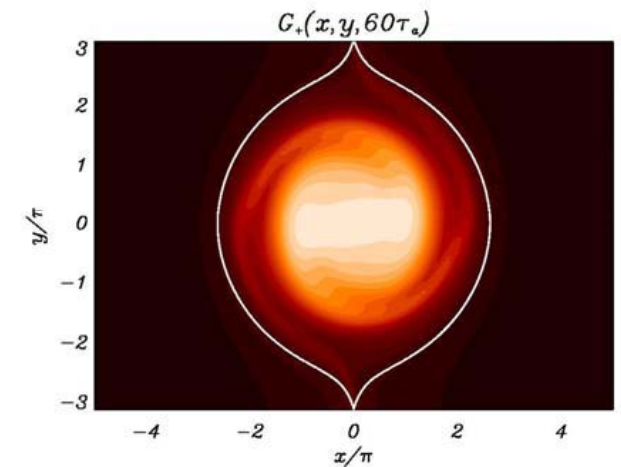
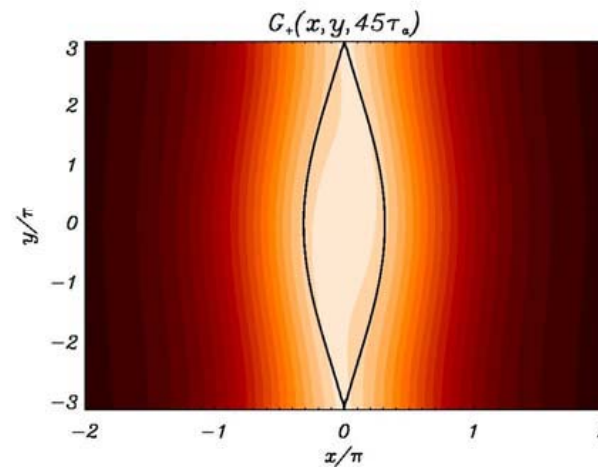
Growth rate comparable to the sawtooth crash time!



Note: the reconnected flux in SH can be measured by the value of the flux function at the X-point, or by the area of the magnetic island.

# 2D limit: phase mixing at $\rho_s \neq 0$

- While the topology of the magnetic flux changes, the topology of the G fields is preserved. While the G fields undergo a **phase mixing** process inside the island, J and U develop a **laminar structure**.



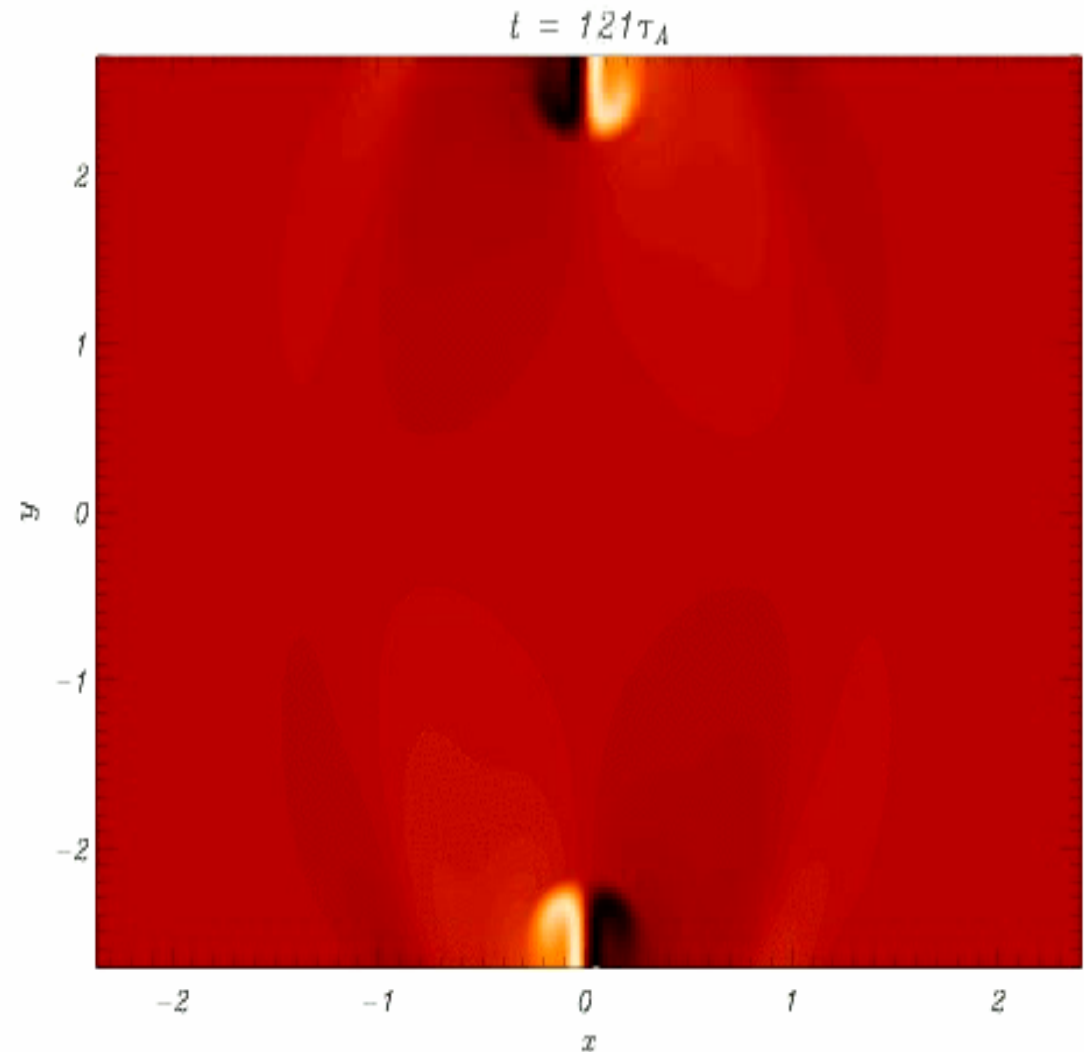
y shift

- Part of the magnetic energy is transferred to small scale structures.
- A new equilibrium state is so accessible in spite of energy conservation for Hamiltonian systems.

D. Grasso *et al.*, PRL 2001.

# 2D limit: KH instability at $\rho_s = 0$

- Occurrence of secondary hydrodynamic (**Kelvin-Helmholtz**) instability during the nonlinear phase in cold electron plasmas can lead to turbulence.
- Two jets start from the X-point and collide at the O-point.
- Disruptions of current density and vorticity layers.

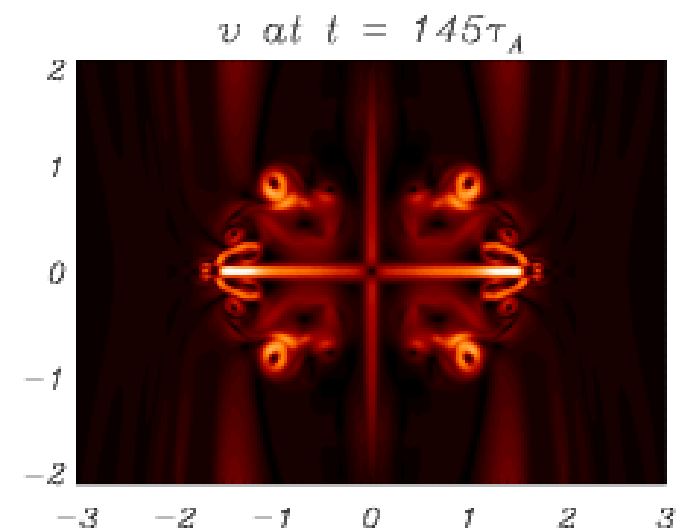
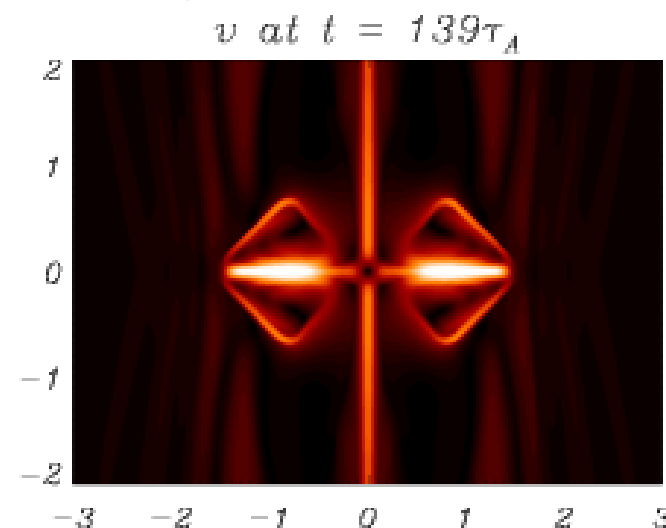
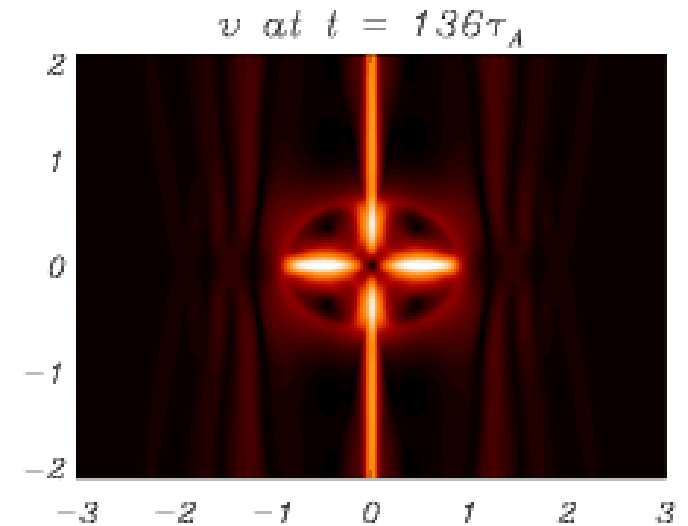
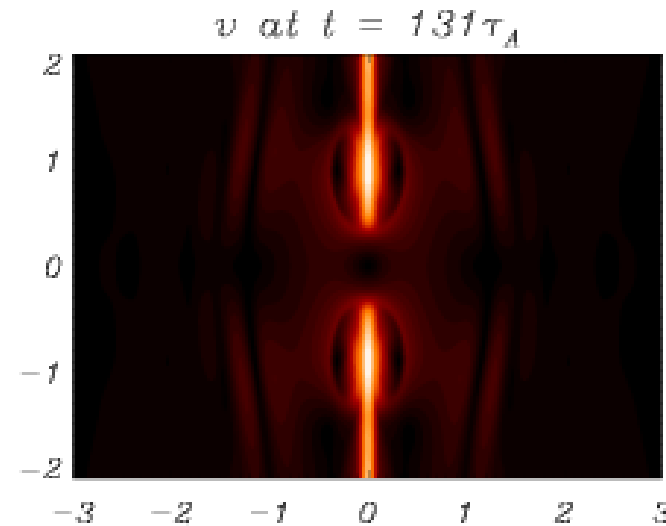


# 2D limit: KH instability

- In the highly nonlinear regime velocity shear develop such that

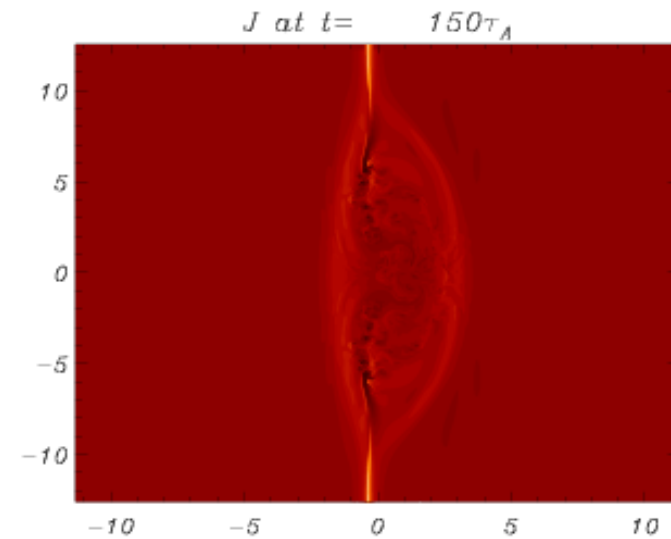
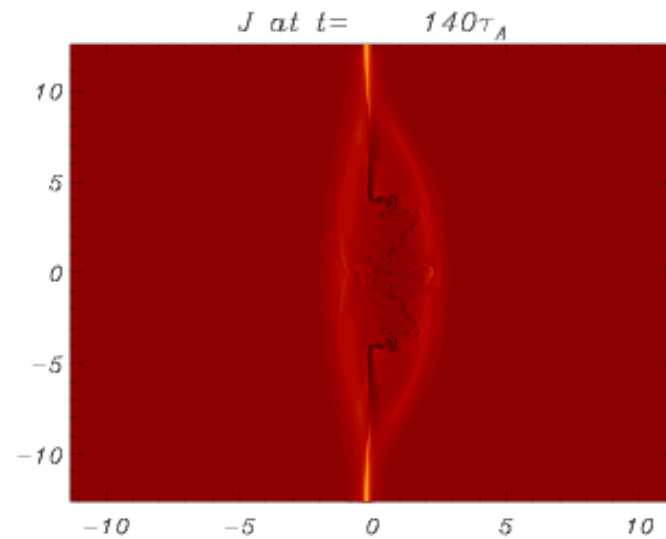
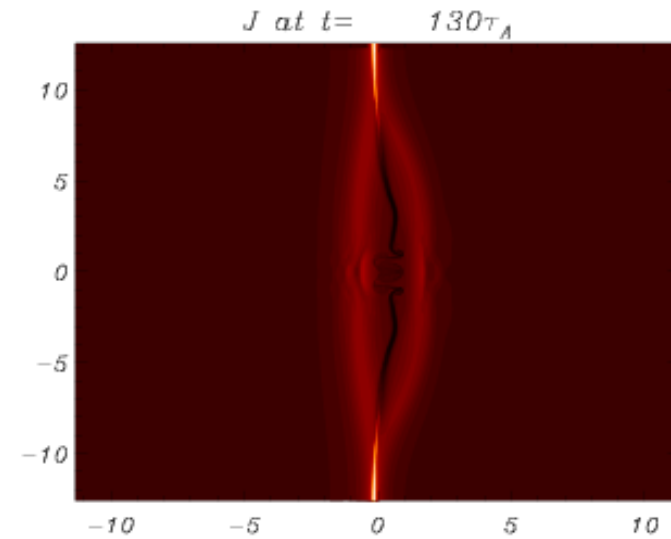
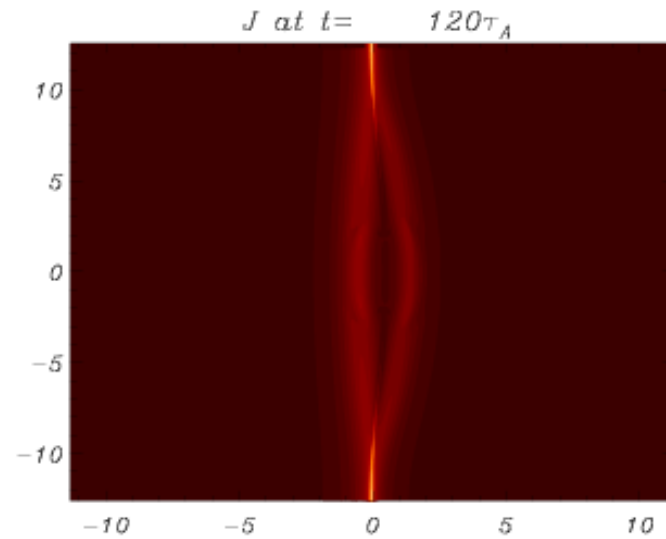
$$[\varphi, U] \approx 10 [J, \psi]$$

so the vorticity equation reduces to  $dU / dt = 0$



# 2D limit: KH instability

Turbulence is confined inside the magnetic island.



# 3D limit: what changes?

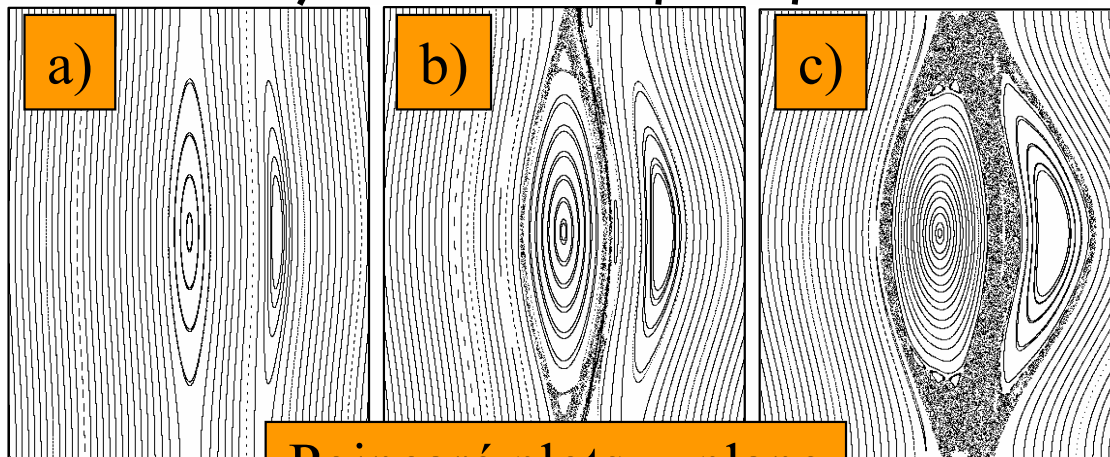
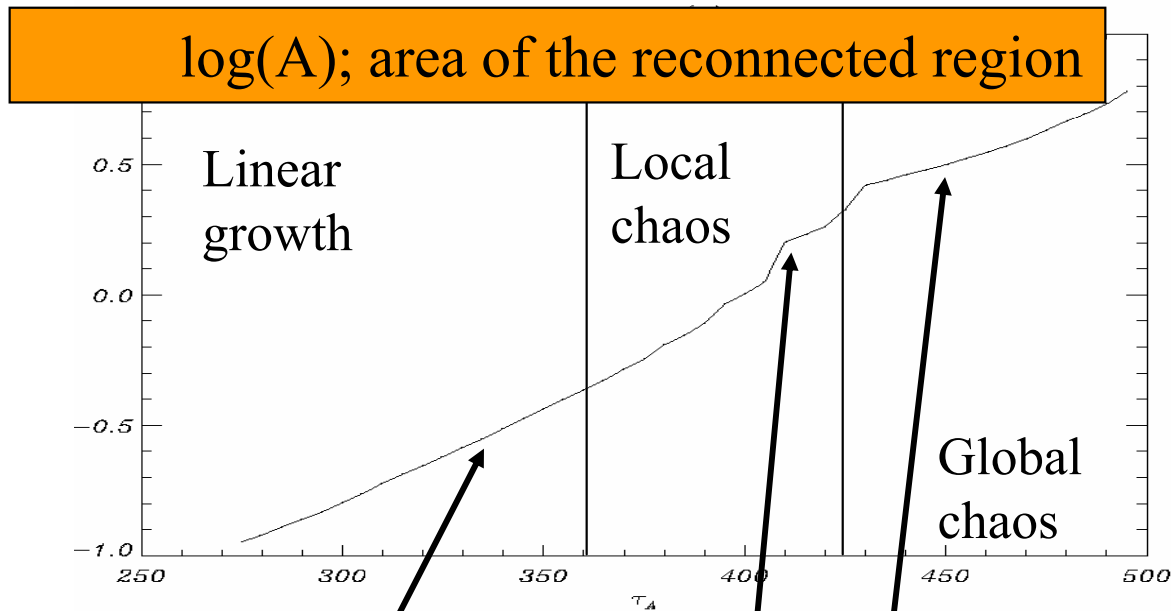
---

- In 3D geometry magnetic field lines don't lie on the surfaces  $\psi = \text{const}$
- $\vec{B} \cdot \nabla \psi \neq 0$  and the Hamiltonian for the magnetic field lines, is no longer integrable. The magnetic field becomes chaotic.
- Magnetic field lines can be represented by the Hamiltonian equations of the following dynamical system:

$$\frac{dx}{dz} = \frac{1}{B_0} \frac{\partial \psi}{\partial y} = \frac{B_x}{B_z}$$
$$\frac{dy}{dz} = -\frac{1}{B_0} \frac{\partial \psi}{\partial x} = \frac{B_y}{B_z}$$

where  $x$  and  $y$  play the role of conjugate variables,  $z$  the role of time and  $t$  is a parameter. Integration of these equations gives Poincaré maps.

# 3D limit: chaotic behavior



Poincaré plots, z plane

- The two modes (1,0) and (1,1) are initially uncoupled
- Chaos develop locally around the separatrix
- Chaos extends globally

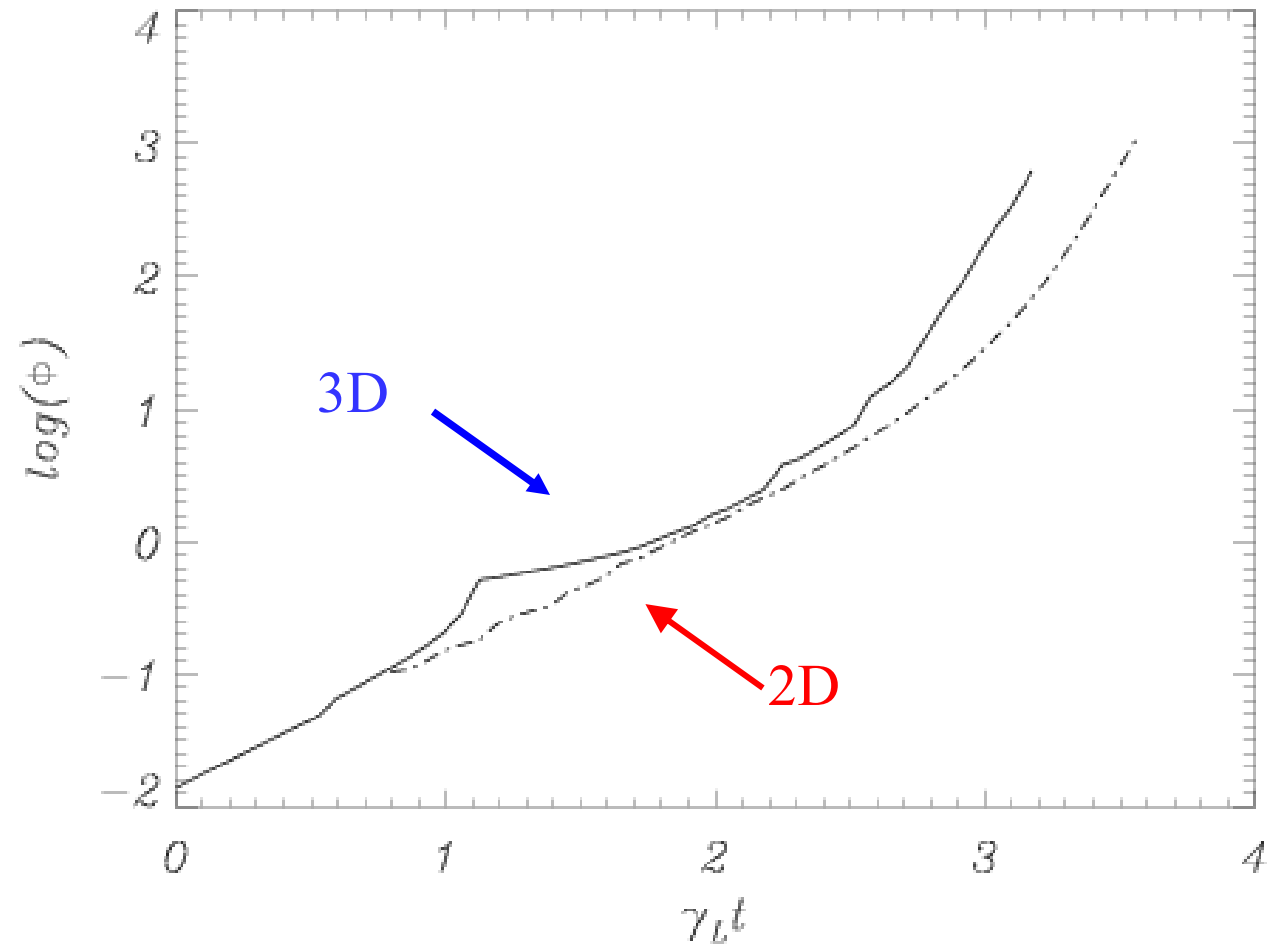
The region with a modified topology enclosed between the regular KAM surfaces represents the 3D extension of the concept of the area of the 2D magnetic island.

**Super-exponential** reconnection rate in the locally stochastic regime

# 3D limit

The magnetic reconnected flux attains a significant value over a time scale of the order of the exponential growth time found in the small amplitude, linear phase.

Growth is faster in the 3D case.

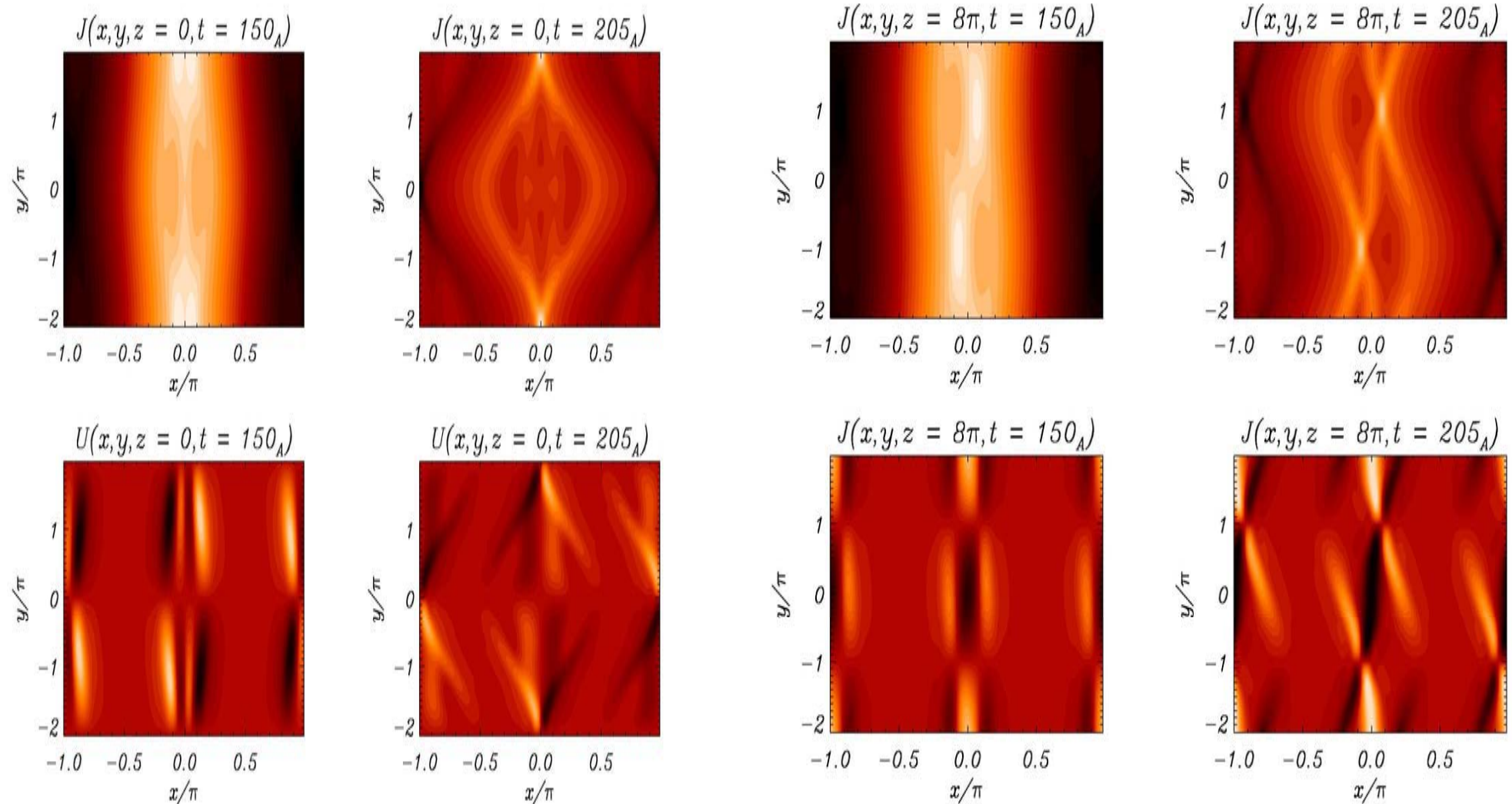


**3D case (1,1/16), (1,-1/16)**  
**2D case (1,1/16)**

# current and vorticity sheets

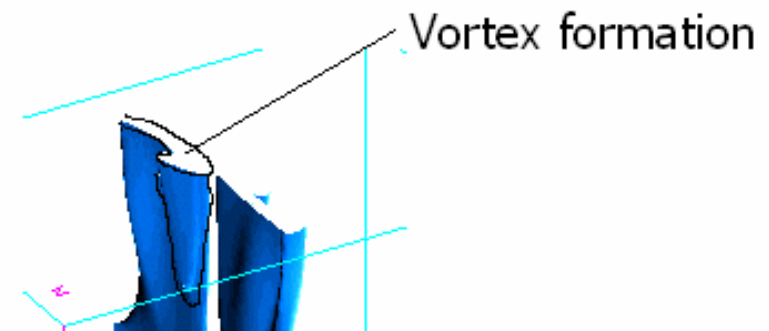
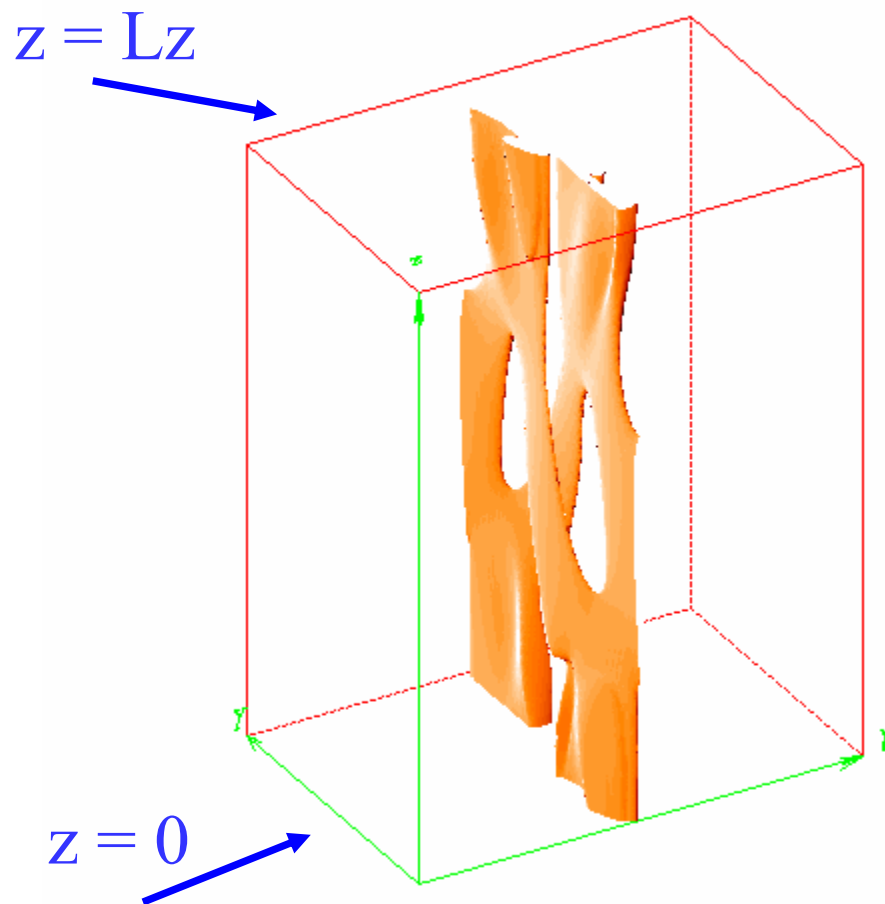
## 3D limit:

## still persist



# 3D limit: KH instability at $\rho_s = 0$

- Strong velocity shear develop
- In the cold electron case, Kelvin-Helmholtz like instabilities develop also in a full 3D setting (*Grasso et al., PoP, 2007*).

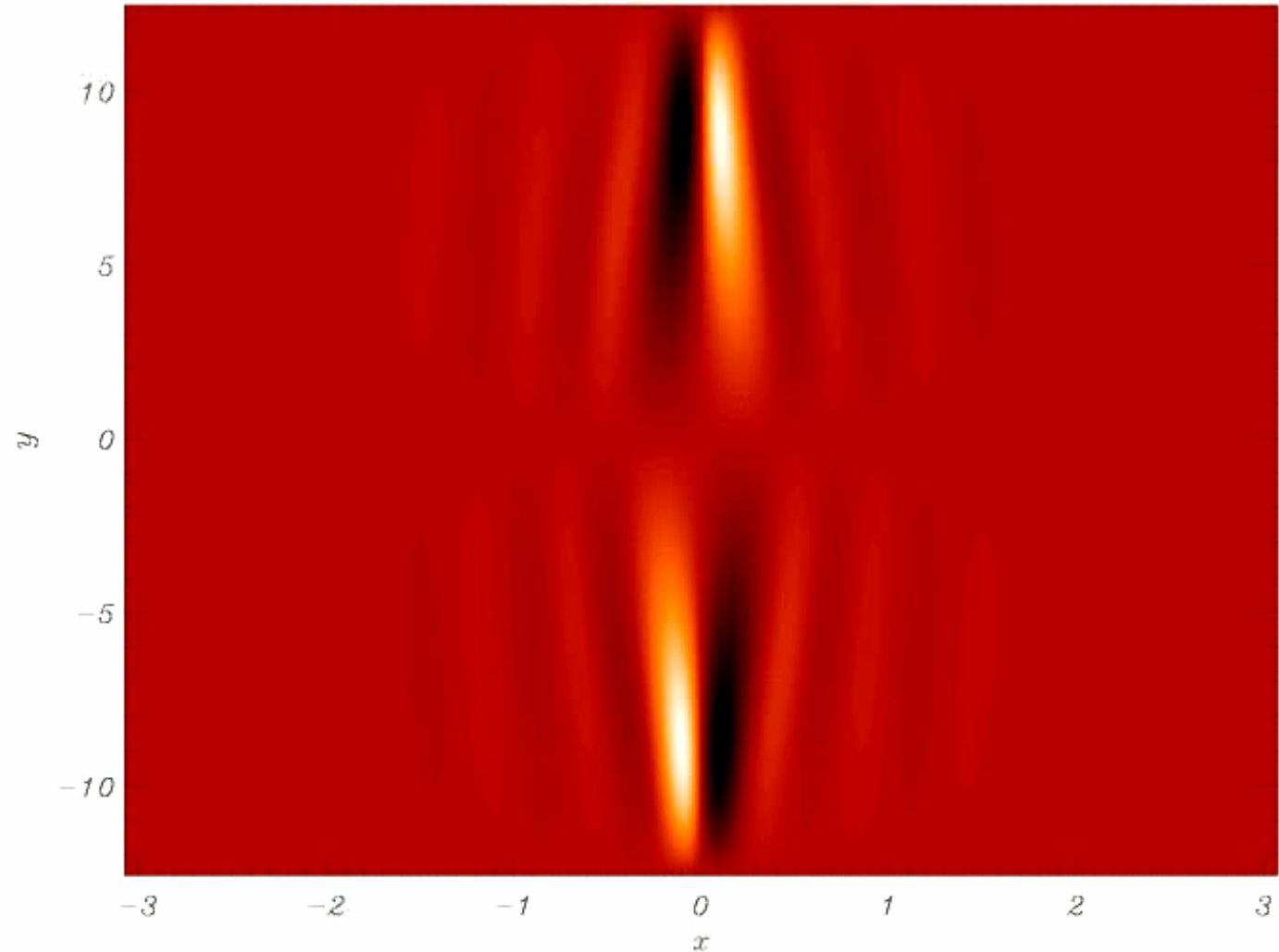


The closer the plane to  $z=0$  ( $z=Lz$ ) the sooner the instability develops. The nonlinear interaction between the helicities produces the most intense shear flows on this plane.

# 3D limit: KH instability

$U(x, y, 0\pi) @ t=110\tau_A$

On each plane there are two jets that generate in correspondence of the  $y$  where the X-points of the dominant perturbed helicities face each other. The strong nonlinear interaction due to the presence of different unstable modes make the dynamics dissimilar from the 2D case.

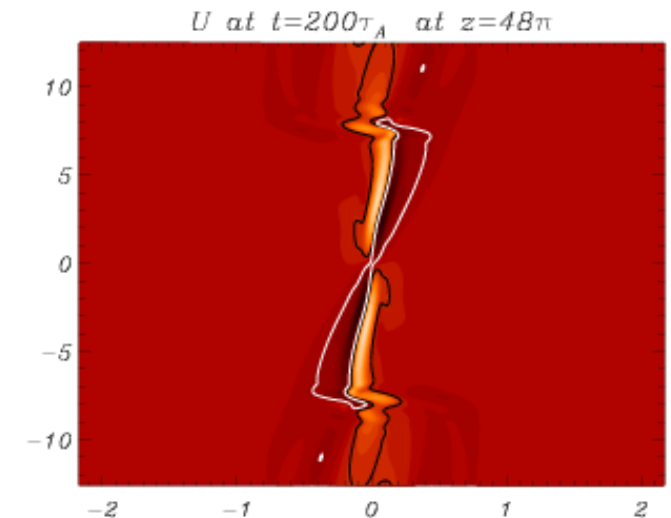
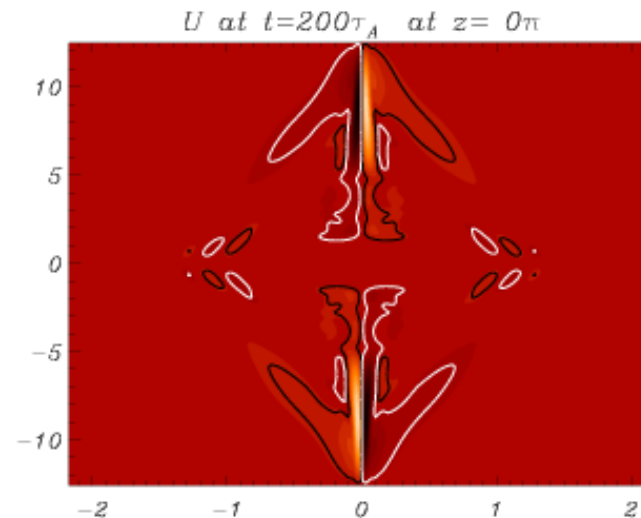
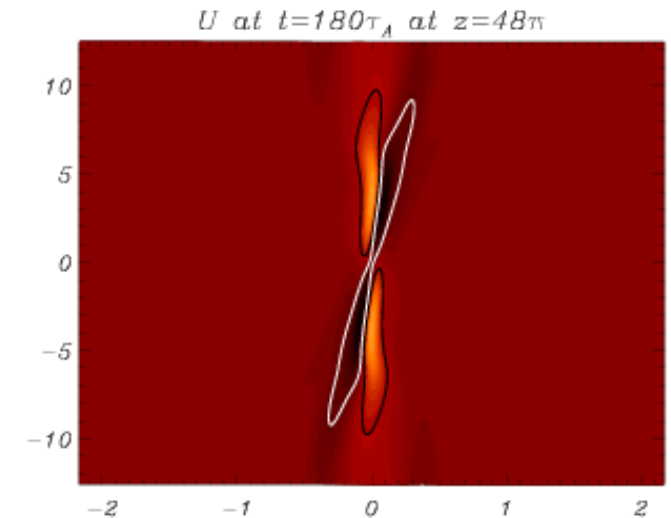
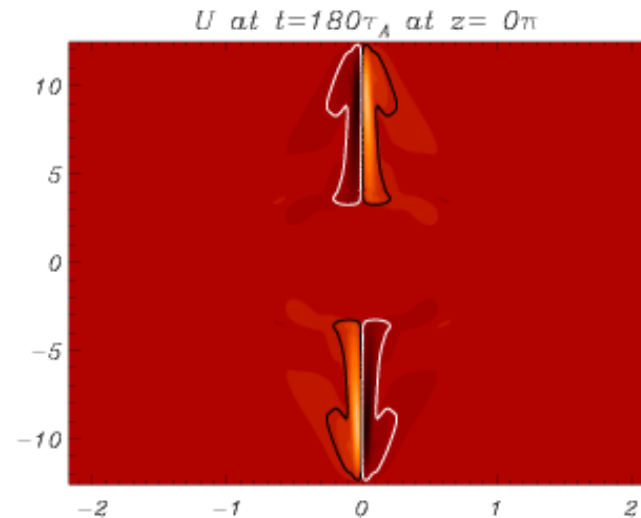


# 3D limit: KH instability

Along the layers that first destabilize we find that the terms of the vorticity equations are in the following relations:

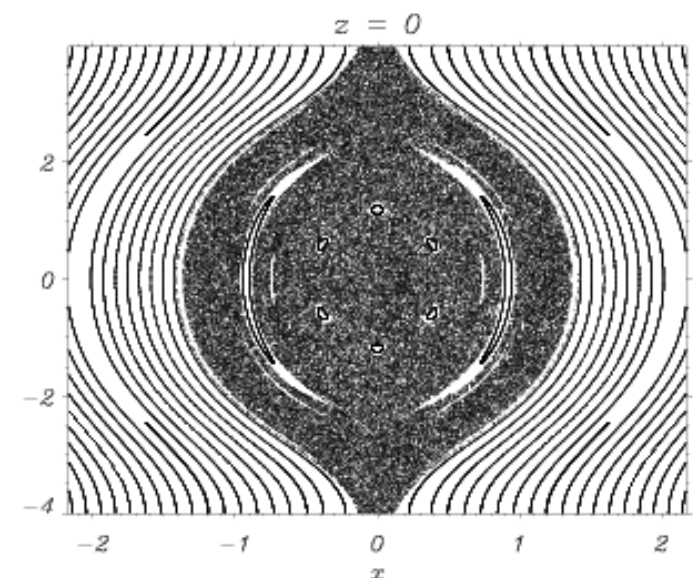
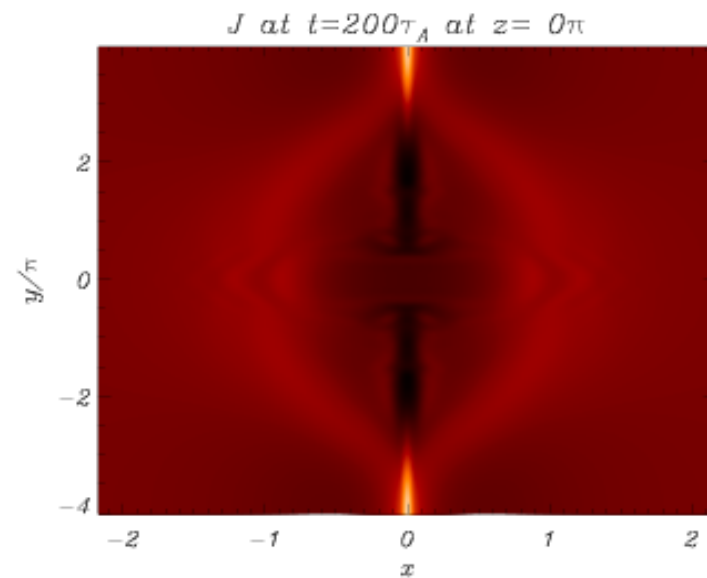
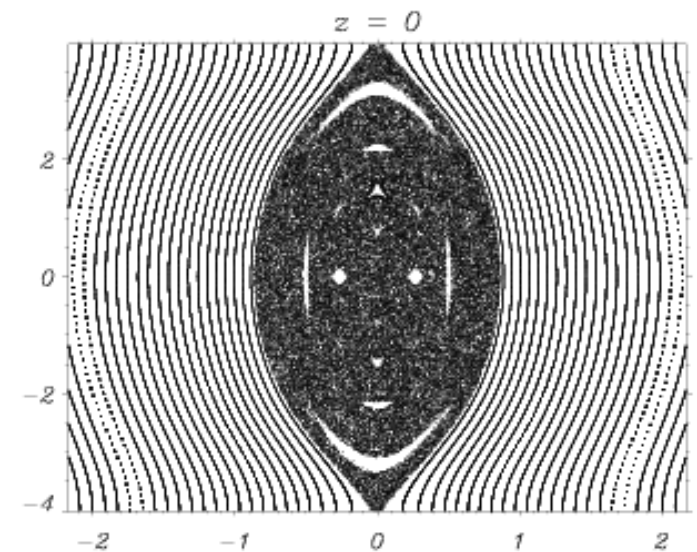
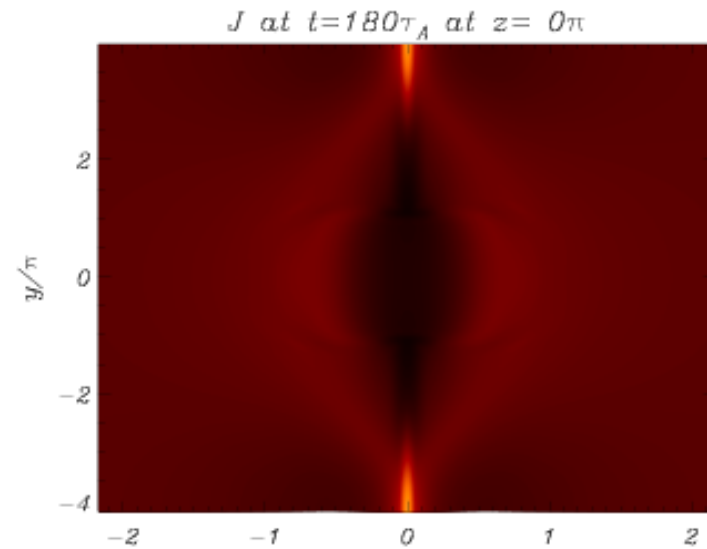
$$[\varphi, U] \approx 10 [J, \psi]$$

$$[\varphi, U] \approx 10 \frac{\partial J}{\partial z}$$



# 3D limit: KH instability

The current density layers undergo the same instability. The area hydrodynamically unstable remains confined within the chaotic area.



# 2D four-field model

- The model by **Fitzpatrick *et al.* (PoP 2004)** is derived from the Hazeltine *et al.* (Phys Fluids 1985), neglecting curvature of the magnetic field and resistivity and including electron inertia.

- Compression of magnetic field along the z-direction is now permitted:

$$B = (B_0 + c_\beta Z)\vec{e}_z + \nabla\psi_{eq}(x) \times \vec{e}_z; \quad c_\beta = \sqrt{\frac{\beta}{1+\beta}}; \quad \beta = \frac{nT}{B^2}$$

- Plasma fluid motion along z-direction is taken into account:

$$\vec{v} = \vec{e}_z \times \nabla\varphi + v\vec{e}_z$$

# 2D four-field model

□ Equations normalized to a macroscopic scale length,  $L$ , and to  $\tau_A$  are:

$$\frac{\partial(\psi + d_e^2 J)}{\partial t} + [\varphi, \psi + d_e^2 J] - d_\beta [\psi, Z] = 0$$

$$\frac{\partial Z}{\partial t} + [\varphi, Z] - c_\beta [v, \psi] + d_\beta [J, \psi] = 0$$

$$\frac{\partial U}{\partial t} + [\varphi, U] - [J, \psi] = 0$$

$$\frac{\partial v}{\partial t} + [\varphi, v] - c_\beta [Z, \psi] = 0$$

$$U = \nabla_\perp^2 \varphi; \quad d_\beta = d_i c_\beta$$

$$J = -\nabla_\perp^2 \psi; \quad c_\beta = \sqrt{\frac{\beta}{1 + \beta}}$$

□ The model reduces to the two-field model

for  $\beta \rightarrow 0$

and  $d_i \rightarrow \infty$

Indeed, in this limit:

$$c_\beta \rightarrow \sqrt{\beta} \rightarrow 0$$

$$d_\beta \rightarrow \rho_s$$

$$E = \int \left( |\nabla \psi|^2 + |\nabla \varphi|^2 + d_e^2 J^2 + Z^2 + v^2 \right) dV$$

# 2D four-field model

□ Again, the above equations can be reformulated as:

$$\frac{\partial D}{\partial t} + [\varphi, D] = 0$$

$$\frac{\partial \omega}{\partial t} + [\varphi, \omega] + d_i^{-2} [\psi, D] = 0$$

$$\frac{\partial T_{\pm}}{\partial t} + [\varphi_{\pm}, T_{\pm}] = 0$$

$$\psi + d_e^2 J = \frac{T_+ + T_-}{2} + \frac{d_e^2}{d_i^2} D$$

$$U = \frac{T_+ - T_-}{2 c_{\beta} d_i d_e} + \omega$$

$$D = \psi + d_e^2 J + d_i v$$

$$\omega = U + Z/\alpha$$

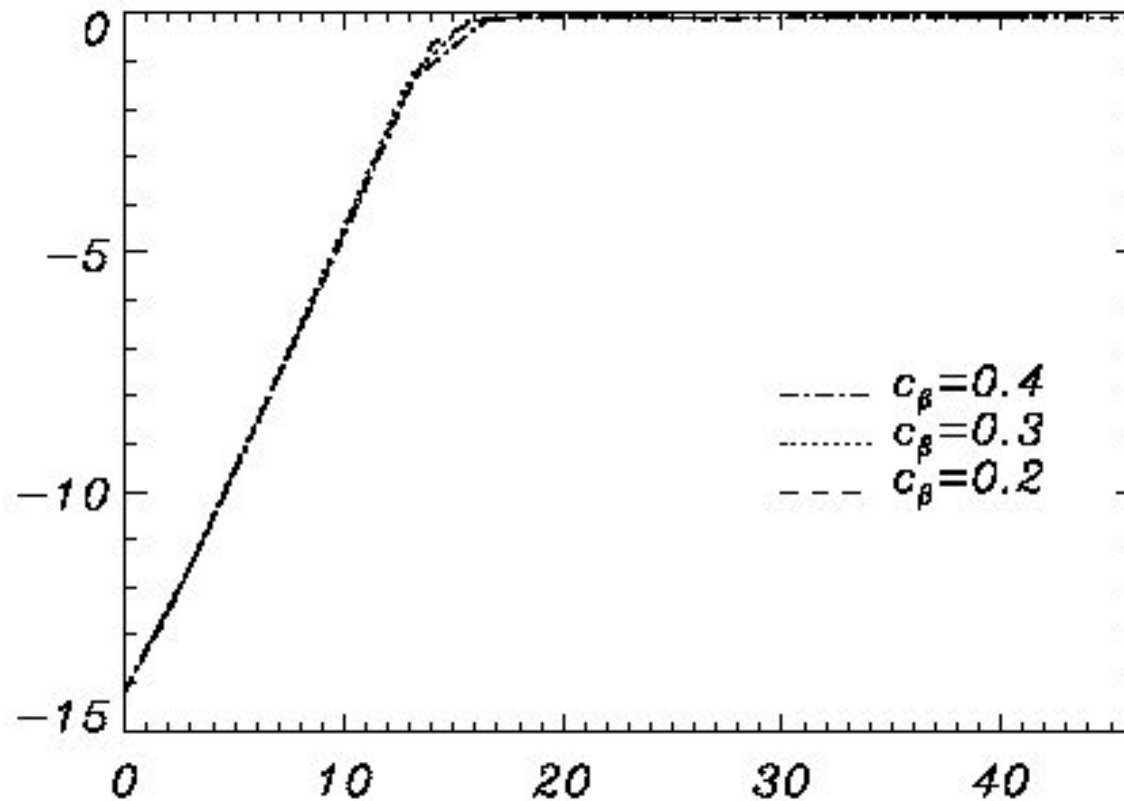
$$\alpha = d_{\beta} + c_{\beta} d_e^2 / d_i$$

$$T_{\pm} = D - \frac{\alpha}{c_{\beta}} v \mp \frac{d_e \alpha^{1/2}}{(d_i c_{\beta})^{1/2}} Z$$

$$\varphi_{\pm} = \varphi \pm \frac{d_{\beta}}{d_e} \psi$$

# 2D four-field model

- Again, the reconnection time is of the order of the inverse growth time.



# 2D four-field model: different regimes

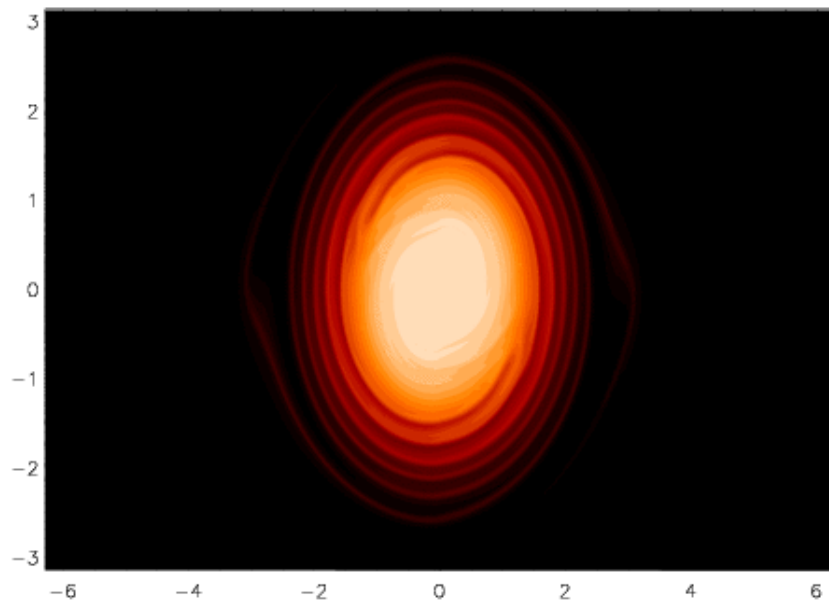
---

- i.  $\beta \rightarrow 0, d_\beta = \rho_s \neq 0 \Rightarrow$  Hot electron case:  
 $T_\pm \rightarrow G_\pm, \quad \omega \rightarrow 0, \quad Z \rightarrow \rho_s U$  laminar regime (phase mixing)
- ii.  $\beta \rightarrow 0, d_\beta = \rho_s \rightarrow 0 \Rightarrow$  Cold electron case:  
turbulent regime (KH instability)
- iii.  $\beta \neq 0, d_\beta \neq 0 \Rightarrow$  Intermediate regime:  
Laminar and turbulent regimes combine (KH + phase mixing)

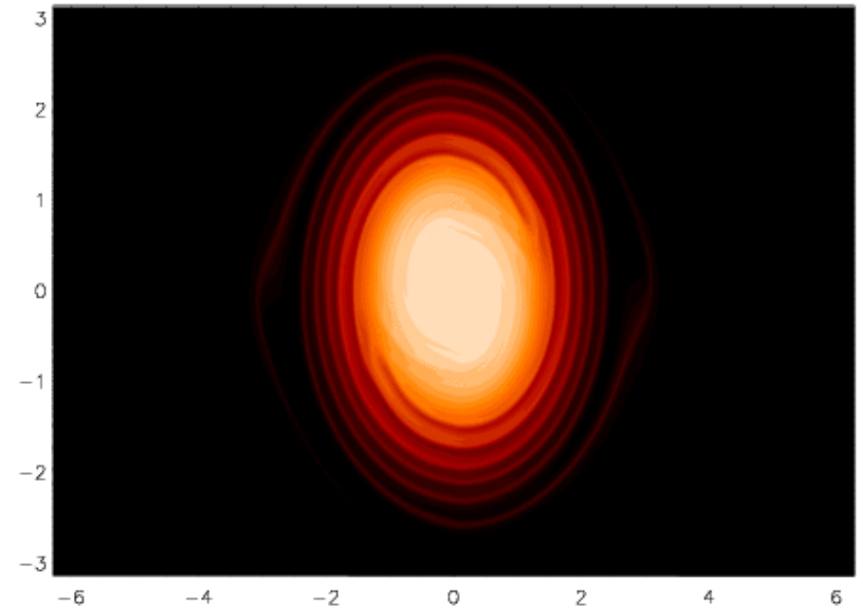
# 2D four-field reconnection: $\beta \neq 0, d_\beta \neq 0$

- The lagrangian invariants  $T_\pm$  do mix in the nonlinear phase

$T_-$

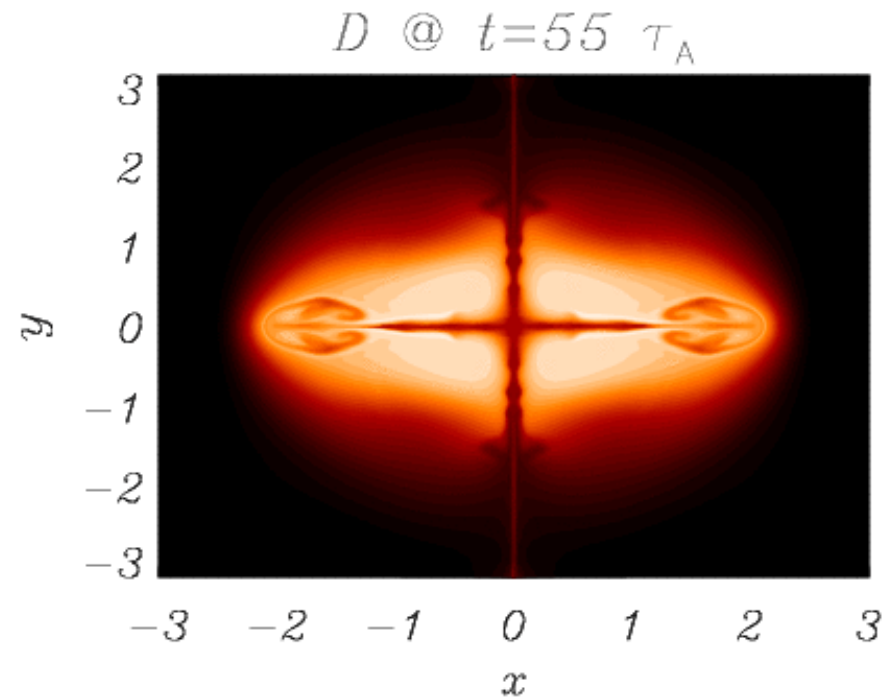
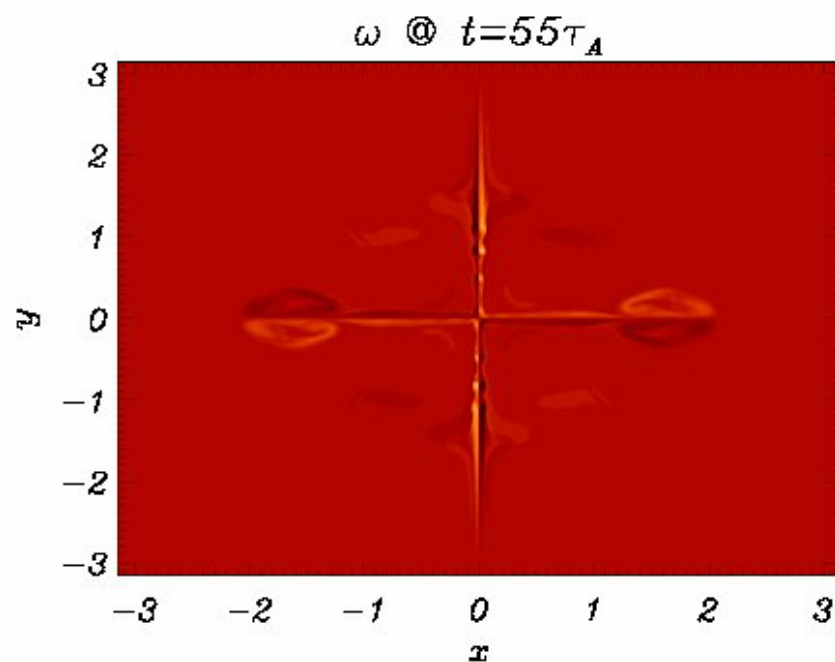


$T_+$



# 2D four-field reconnection: $\beta \neq 0, d_\beta \neq 0$

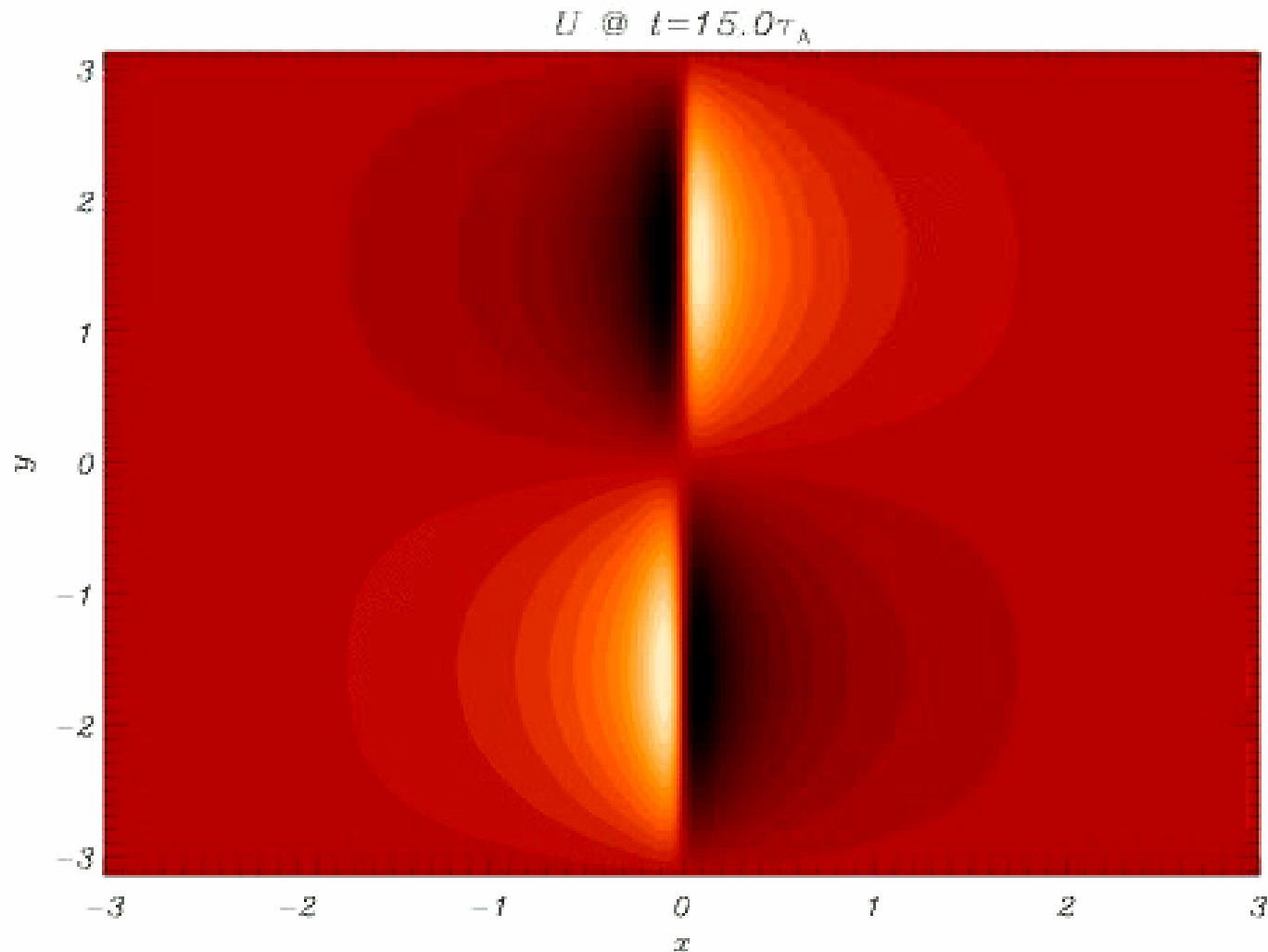
- The new invariants  $D$  and  $\omega$  do not undergo phase mixing



- Note:  $\omega$  is related to the  $Z$  field, which is physically responsible for compression of the magnetic field along the ignorable direction.

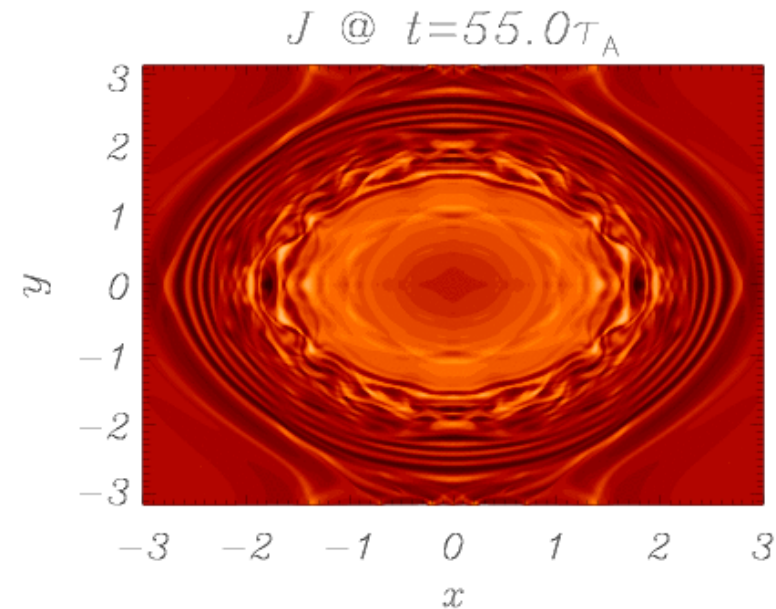
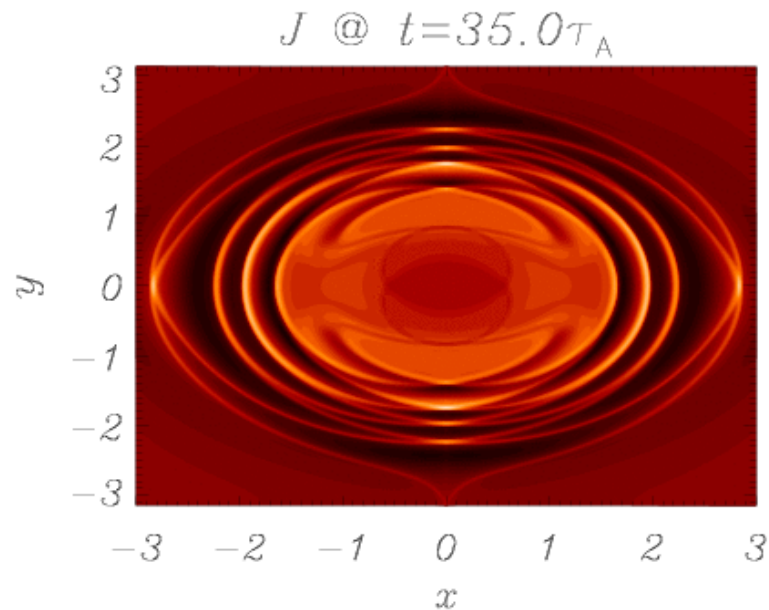
# 2D four-field reconnection: $\beta \neq 0, d_\beta \neq 0$

- Velocity shear develops and is subject to hydrodynamic instabilities



# 2D four-field reconnection: $\beta \neq 0, d_\beta \neq 0$

- Due to the different generalized connections that constrains the plasma the current density has a different structure from the vorticity.



$$J = \frac{T_+ + T_-}{2 d_e^2} - \frac{\psi}{d_e^2} + \frac{1}{d_i^2} D$$

$$U = \frac{T_+ - T_-}{2 c_\beta d_i d_e} + \omega$$

Absent in the two-field limit

# Conclusions

---

- Two-field magnetic reconnection:
  - 1) Quasi-explosive behavior in 2D and 3D settings
  - 2) Phase mixing process for finite electron temperature
  - 3) Kelvin-Helmholtz instability in the cold electron limit both in 2D and 3D settings
  
- Four-field magnetic reconnection:
  - 1) Quasi-explosive behavior in 2D is confirmed
  - 2) The topological constraints relax allowing for phase mixing and Kelvin-Helmholtz instability to coexist in a warm electron plasma

# Open problems

---

- Connection with the zero guide field limit
- Role of pressure of anisotropy
- FLR effects and kinetic effects
- Inclusion of 3D effects in the four-field model
- .....